Revista de metalurgia

Estudio de la función de los diboruros en la nucleación heterogénea del aluminio(•)

O.M. Suárez*

Resumen

En el presente trabajo se revisa el papel de los diboruros de titanio y aluminio en la nucleación del aluminio y se evalúa la estabilidad de dichos boruros en presencia de fases de tri-aluminiuros de titanio y aluminio líquido. Los boruros de alta temperatura se retuvieron mediante solidificación rápida y se estudiaron empleando técnicas diferentes complementadas con microscopía electrónica de barrido. La reactividad de los boruros se analizó en un par de difusión en contacto con tri-aluminiuro de titanio puro. La presente investigación propone que un diboruro ternario actúa como principal partícula catalítica en la cristalización de aleaciones de aluminio con grano refinado.

Palabras claves Nucleación heterogénea. Afinadores de grano. Aluminio. Boruros. Solidificación. Solidificación rápida.

A study on the role of diborides in the heterogeneous nucleation of aluminium

Abstract

The intangible role of titanium and aluminium diborides in the nucleation of aluminium was re-examined. Two different techniques, complemented with scanning electron microscopy, allowed determining the stability of the diborides in the presence of titanium trialuminides and liquid aluminium phases. Through rapid solidification quenching the high temperature diborides were retained and studied. Then, in a diffusion couple, the reactivity of such diborides was tested in contact with pure titanium trialuminide. It is proposed that a ternary diboride acts as the main catalytic particle in the crystallization of aluminium alloys with refined grains.

Keywords Heterogeneous nucleation. Aluminium grain refiners. Borides. Solidification. Rapid solidification.

1. INTRODUCTION

Heterogeneous nucleation as a method to control the formation of specific phases upon solidification of metallic materials has been the subject of numerous investigations for many years. This applies to different materials such as the nucleation of graphite in spheroidal graphite cast iron[1 y 2] or the nucleation of primary silicon in hypereutectic Al-Si alloys[3]. In the case of aluminium grain refiners, the role of titanium and boron has been widely discussed and researched for many years[4]. As an instance of controlled heterogeneous nucleation, aluminium grain refiners consist of mainly commercial alloys containing Al_3Ti and titanium diboride particles[5] as well as silicon impurities[6]. For example, the effectiveness of these grain refiners was assessed by means of the controlled addition of nucleant particles, single nucleation substrates, or through the subdivision of the liquid alloy into fine droplet dispersion[7], a technique also extended to other casting materials such as cast irons[8].

While the catalytic effect of the Al_3Ti particles as substrates for aluminium (Al) nucleation is well known, the true role of TiB_2 particles present in Al-Ti-B grain refiners is still under discussion. It is clear, however, that Al-Ti master alloys containing boron are much more effective than Al-Ti master alloys without boron[9].

Additionally, the nucleation process of aluminium is a phenomenon inherently kinetics-related which can mask the most careful thermodynamic studies. For instance, dissolution

(•) Trabajo recibido el día 29 de agosto de 2003 y aceptado en su forma final el día 25 de mayo de 2004.
(*) Dpto. de Ingeniería General, Universidad de Puerto Rico -Mayagüez. P.O. Box 9044. Mayagüez 00681. Puerto Rico.

processes after the addition of the grain refiners play an important role in the process as shown by the addition of molten Al-Ti-B master alloys to molten aluminium[10]. Hence, the stability of the titanium diborides in aluminium melts containing titanium might not be accurately modeled by means of thermodynamic simulations only. These strong interactions were observed by Schumacher, *et al.*, along with α-Al nucleation on the basal faces of TiB_2 particles coated with Al_3Ti in laboratory conditions[11]. On the other hand, *Zupanic, et al* indicated that in as-cast Al-Ti-B alloys "apparently" pure, TiB_2 and AlB_2 coexist even after 1000 h exposure at 800 °C, and that no $(Al,Ti)B_2$ was observed[12]. The same authors added that "it seems very likely that the mixed diboride $(Al,Ti)B_2$ is not a thermodynamically stable phase in the aluminium rich corner of the Al-Ti-B system".

From those studies two common arguments can be extracted. First, there is a general agreement about the influence of kinetics in the phase formation during solidification of ternary Al-Ti-B alloys. This kinetic effect hampers a clear understanding about the appearance and role of TiB_2 and AlB_2 particles or the possible ternary $(Al,Ti)B_2$. This leads to the second argument about the existence of such a ternary diboride. Due to kinetic effects, experimental corroboration of thermodynamic modeling of the system may be very restricted by even minor artifacts or the presence of small levels of impurities like silicon. This factor was previously addressed by producing high purity ternary Al-Ti-B alloys and comparing these results with commercial master alloys[13].

Recently Tee *et al.* [14] in an attempt to produce aluminium matrix composites reinforced with TiB_2 particles observed the unavoidable presence of Al_3Ti particles. This trialuminide is a brittle phase that hinders further development of aluminium matrix composites containing titanium since they can crack upon manufacturing. On the other hand, diborides do provide a beneficial strengthening effect. The presence of AlB_2 particles well embedded into the aluminium matrix in a fractured Al-B composite indicates the strong bonding between aluminium and AlB_2, which further validates the proposed explanation that those diborides are catalytic substrates for aluminium nucleation[15].

To address the stability of borides in contact with liquid aluminium it is necessary to retain the high temperature microstructure through specialized quenching experiments and trace its evolution during and after solidification of the α-Al phase, through completion. This can be accomplished by using diffusion couples in the Al-Ti-B ternary system and complementary quenching experiments during the formation of the (Al) phase on the catalytic substrates. By employing a combination of those techniques this paper proposes an alternative scenario which would overcome the lack of adequate information on the actual role of the diborides in the nucleation of aluminium.

2. EXPERIMENTAL PROCEDURE

Experimental alloys were prepared in an arc-melting system by alloying high-purity pieces of Al_3Ti with Al (99,9999) and binary Al-B alloys. These alloys were used to further study the stability of TiB_2 in contact with liquid aluminium and in the presence of large amounts of Al_3Ti phase.

To study the stability of aluminium diboride and Al_3Ti when both phases are present in a ternary system, diffusion couples were used. A diffusion couple was prepared with two small pieces of pure Al_3Ti and a binary Al - B alloy containing 7.08 at % B, which were polished and pressed against each other and held together by alumina-coated tungsten clamps. The diffusion couple was held at 610 °C for 120 h in an evacuated quartz capsule to prevent oxidation. After annealing, the couple was transversally cut by means of a diamond wheel, polished and observed unetched in a scanning electron microscope (SEM). This microscope was equipped with a highly sensitive backscattered electron detector and an energy dispersive spectroscopy (EDS) analyzer, which allowed to determine the diffusion profile across the interface. The results of the diffusion couple studies were then compared with the outcome of previous investigations that involved commercial and experimental Al-Ti-B alloys. For these latter experiments a droplet emulsion technique (DET) allowed to discriminate between potent (catalytic) substrates and inactive particles during the nucleation of the α-Al phase[16].

Some of these experimental alloys were splat quenched from the liquid in order to retain the high temperature diborides. This splat-quenching technique consisted of RF levitation and melting of the sample and subsequent dropping and rapid solidification by clapping two flat copper anvils together as the dropping sample is passing in between. An electronic eye detects the falling

molten sample and activates the anvils. A schematic diagram of the splat quenching apparatus is shown in figure 1. The temperature attained just before dropping the sample is about 1800 °C and the cooling rate is roughly 1000 °C·s^{-1}.

A differential thermal analysis (DTA) apparatus provided additional information related to thermal evolution of the microstructure. This DTA unit allowed determining accurate nucleation temperatures of the α–Al phase as well as of Al_3Ti when the experimental results where coupled with X-ray difraction analyses.

3. RESULTS

In figure 2, a scheme of the Al-rich corner of the Al-Ti-B phase diagram at room temperature is shown to indicate the experimental alloys used to study the effect of boron. Of all of them, only the alloys containing 86.7 at % Al, 12.5 at % Ti and 0.8 at % B ($Al_{86.7}Ti_{12.5}B_{0.8}$), and 96.6 at % Al, 2.9 at % Ti and 0.5 at % B ($Al_{96.6}Ti_{2.9}B_{0.5}$) are reported in the present article for the sake of conciseness. The $Al_{86.7}Ti_{12.5}B_{0.8}$ alloy was prepared to obtain a large volume fraction of trialuminide and to observe the effect of the diboride in contact with or nearby that phase.

The as splat-quenched microstructure of the alloy $Al_{86.7}Ti_{12.5}B_{0.8}$ is shown in figure 3 using

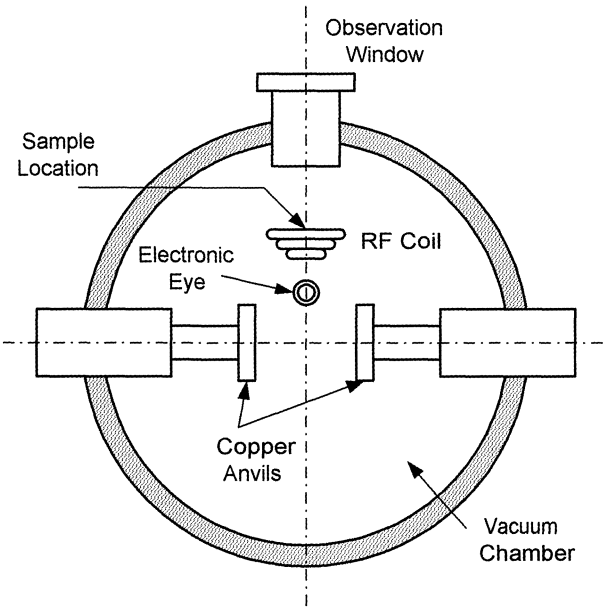

Figure 1. Scheme of the splat quenching machine used to study the high temperature behavior of the Al-Ti-B ternary alloys.

Figura 1. Esquema de la máquina de temple rápido utilizada para el estudio del comportamiento a alta temperatura de las aleaciones ternarias Al-Ti-B.

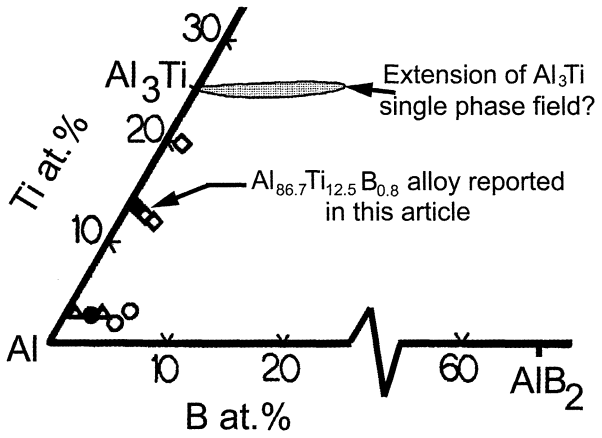

Figure 2. Al-rich corner of the Al-Ti-B phase diagram indicating the composition of several alloys investigated. The hypothetical extension of the Al_3Ti single phase field is discussed later in the present article.

Figura 2. Vértice rico en aluminio (Al) del diagrama Al-Ti-B indicando la composición de varias de las aleaciones investigadas. La extensión hipotética de un campo monofásico Al_3Ti se analiza más adelante en el presente trabajo.

backscattered electrons. The light gray phase corresponds to the Al_3Ti phase, as indicated by EDS analysis surrounded by α-Al phase in solid solution with titanium (Ti) due to liquid quenching. The diborides (labeled as B) represent the largest, distinguishable phase with faceted edges, embedded well within the sample. Unmistakably, they were already solid before the

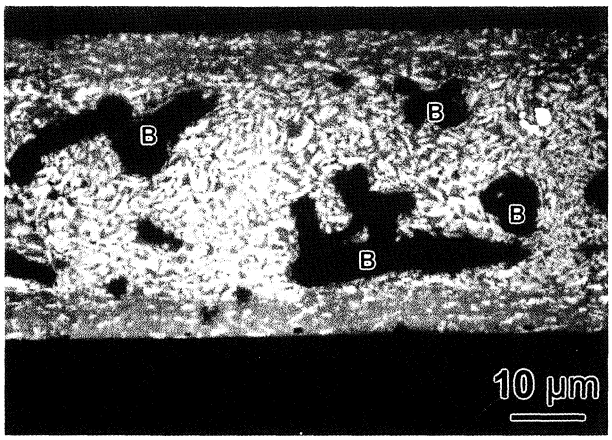

Figure 3. Backscattered electron image of the cross section of alloy $Al_{86.7}Ti_{12.5}B_{0.8}$, as splat-quenched. Borides are labeled as B, while the light gray phase corresponds to Al_3Ti phase according to EDS analysis. The remaining gray phase is the α-Al phase supersaturated with titanium (Ti) due to liquid quenching.

Figura 3. Imagen de electrones retrodispersados de la sección transversal de la aleación $Al_{86,7}Ti_{12,5}B_{0,8}$ en estado templado. Los boruros están identificados como B, mientras que la fase gris clara corresponde a Al_3Ti de acuerdo con el análisis EDS. La fase restante gris oscura es Al-α con titanio (Ti) en solución sólida provocado por el temple desde el estado líquido.

molten specimen was dropped between the anvils showing the high temperature stability (high melting point) of diborides. Complementary XRD and EDS analyses showed the composition of these phases to correspond to TiB_2 as later verified by XRD analysis[16].

In order to study the evolution of the ternary $Al_{86.7}Ti_{12.5}B_{0.8}$ alloy upon normal cooling (5 °C·min^{-1} from the melt), the corresponding DTA thermogram is shown in figure 4a and b. The upper plot (Fig. 4a) shows the whole curve in order to include the formation temperature of the Al_3Ti phase. The lower plot (Fig. 4b) corresponds to a close-up of the previous curve within the aluminium phase solidification range.

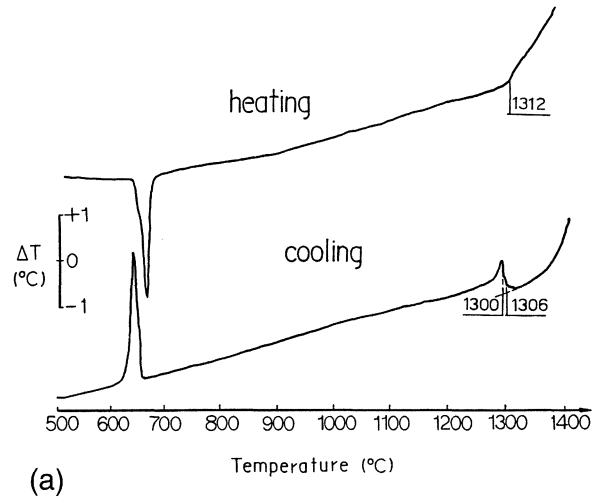

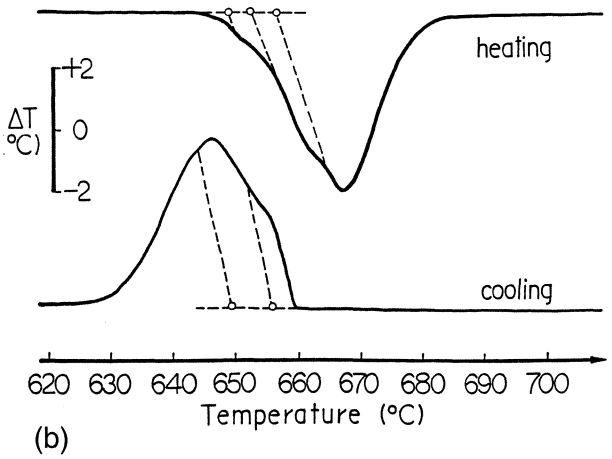

Figure 4. DTA thermogram obtained for the alloy $Al_{86.7}Ti_{12.5}B_{0.8}$. Heating and cooling rates were set up at 5 °C·min^{-1}. a) Full curve displaying the remelting and solidification temperatures of Al_3Ti; b) Close-up of the curves in the aluminium solidification temperature range.

Figura 4. Termograma DTA obtenido para la aleación $Al_{86.7}Ti_{12.5}B_{0.8}$. Las velocidades de calentamiento y enfriamiento se fijaron en 5 °C·min^{-1}. a) Curva completa mostrando las temperaturas de refusión y solidificación de Al_3Ti; b) Detalle de las curvas correspondientes a la fusión y solidificación de la fase aluminio.

After the DTA studies, the $Al_{86.7}Ti_{12.5}B_{0.8}$ alloy was observed in a SEM using mixed backscattered and secondary electron imaging (BEI + SEI) mode in order to improve contrast among different phases. In figure 5, the resulting microstructure is shown, revealing the consistent association of diboride particles (labeled B) with Al_3Ti phase. Due to the large fraction of trialuminide present, it is possible to observe diborides near the Al_3Ti chunky particles (shown as bright in the BEI + SEI photograph), producing cracks on the brittle trialuminide. This detail shows the high reactivity of the diboride, which a further EDS analysis reveals as being $Al_xTi_{1-x}B_2$ or $(Al,Ti)B_2$ with variable levels of aluminium and titanium throughout the sample. The appearance of aluminium in the diboride composition at room temperature should then be traced back to the phase transformations occurring before and during the α-Al phase solidification range.

A sample of the alloy $Al_{96.6}Ti_{2.9}B_{0.5}$ was emulsified using a droplet emulsification technique (DET) described in a previous research[6,7 y 13]. The emulsification process allowed to isolate particles that are potential catalytic substrates by subdividing the melt into fine droplets. When

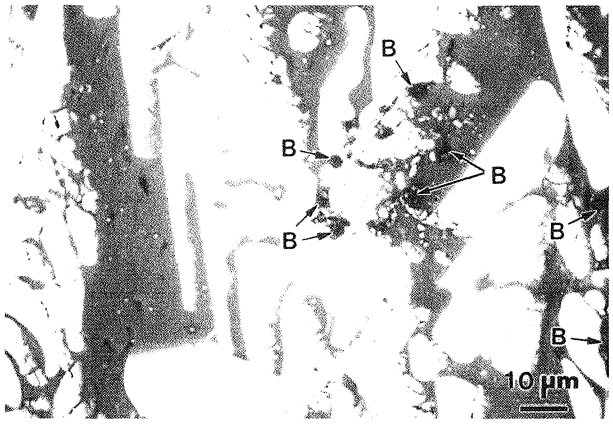

Figure 5. General aspect of experimental $Al_{86.7}Ti_{12.5}B_{0.8}$ alloy after DTA cycling, as observed using BEI + SEI mode depicting the formation of three phases: Al (gray phase), Al_3Ti (bright phase), and the diborides (dark gray particles labeled B). Note that the small diborides are often associated with adjacent cracked Al_3Ti phase.

Figura 5. Aspecto general de la aleación experimental $Al_{86.7}Ti_{12.5}B_{0.8}$ tras realizar los ciclos DTA como se observan en modo BEI + SEI evidenciando la formación de tres fases: Al (fase gris), Al_3Ti (fase brillante), y los diboruros (partículas grises oscuras indicadas como B). Nótese que los pequeños diboruros aparecen frecuentemente asociados a la fase adyacente Al_3Ti agrietada.

subjected to DTA analysis this emulsified alloy presented the same exothermic events upon cooling through the aluminium solidification range as those observed in the alloy $Al_{86.7}Ti_{12.5}B_{0.8}$ (Fig. 6). The main difference is the intensity of the first two

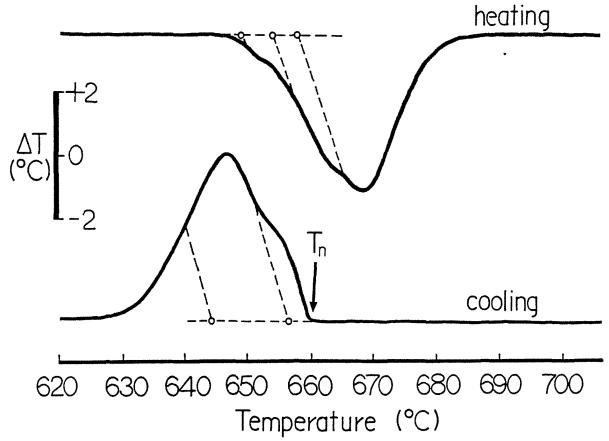

Figure 6. DTA thermogram obtained for an emulsified sample of experimental alloy $Al_{95.1}Ti_{2.9}B_{2.0}$. Heating and cooling rates were set up at 5 °C·min^{-1}. T_n indicates the onset of nucleation upon cooling.

Figura 6. Termograma DTA obtenido para una muestra emulsificada de la aleación experimental $Al_{95.1}Ti_{2.9}B_{2.0}$. Las velocidades de calentamiento y enfriamiento fueron fijadas en 5 °C·min^{-1}. T_n indica la temperatura de comienzo de nucleación durante el enfriamiento.

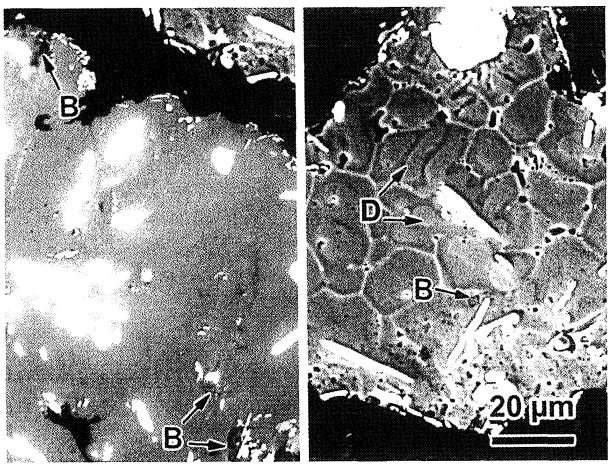

Figure 7. BEI + SEI micrographs of an experimental $Al_{96.6}Ti_{2.9}B_{0.5}$ as emulsified and quenched from temperature T_n (Fig. 6), showing Al_3Ti (white) on an Al matrix (gray) and very small boride particles (labeled as B). D indicates location of dendritic formation on seemingly *active* trialuminides. (a) unetched sample, (b) etched sample.

Figura 7. Micrografías BEI+SEI de una aleación experimental $Al_{96.6}Ti_{2.9}B_{0.5}$ emulsificada y templada desde la temperatura T_n (Fig. 6), mostrando Al_3Ti (blanco) en una matriz de Al (gris) y partículas de boruros muy pequeñas (indicadas como B). D indica la localización de una formación en trialuminiuros aparentemente activos. (a) muestra sin ataque químico, (b) muestra con ataque químico.

exothermic peaks due to the larger (Al) phase volume present in the alloy $Al_{96.6}Ti_{2.9}B_{0.5}$ as compared to $Al_{86.7}Ti_{12.5}B_{0.8}$. A different set of $Al_{96.6}Ti_{2.9}B_{0.5}$ samples were quenched at the onset of the first exothermic signal (labeled T_n). Figure 7a and b display two BEI + SEI micrographs of the emulsified and quenched alloy with and without etching[13]. Furter etching revealed catalytic aluminide particles which promoted early formation of α-Al phase (dendritic or offshoot shapes labeled as D in the micrograph of figure 7b), while the remaining trialuminides are surrounded by a featureless solid α-Al phase.

In Figure 8a, b and c the diffusion couple interface is shown. In figure 8a, the Al_3Ti phase is on the left side of the diffusion couple whereas the Al-B binary alloy is on the right side. The original interface has been disturbed by the presence of AlB_2 particles present in the Al-B binary alloy. The reactivity between both sides is evident in figure 8b where diborides (dark gray particles) appear embedded into the Al_3Ti phase. Small, denser particles (light gray, labeled T) were also found associated with diborides. Further EDS analysis indicate they have a composition closer to Al_2Ti. In figure 8c, the close contact between diborides and the trialuminide is even more evident, as diborides appeared well embedded into the Al_3Ti phase. Figure 9 displays boron, titanium and aluminium concentration profiles across the interface for the diffusion couple Al-7.80 at % B alloy (left side) and Al_3Ti (right side) annealed at 610 °C for 120 h. Additional EDS analysis of diboride particles indicated variable amounts of titanium (Ti) and aluminium (Al) ranging from 0 at % Ti and 33 at % Al in diborides in the Al-B side, away from the interface to 15 at % Ti and 18 at % Al in diboride particles embedded in the Al_3Ti phase. This was further shown by different levels of gray of BEI images.

4. DISCUSSION

When comparing the exotherms in the (Al) phase solidification range in figure 4b and 6, there is a strong similarity in terms of their thermal evolution. Based upon quenching study results in the present and prior investigations[16], the signals represent a convolution of three exothermic reactions, the first one (from right to left) being the early formation of α-Al on the most potent (or catalytic) substrates, as there is essentially no undercooling with respect to (Al) melting point

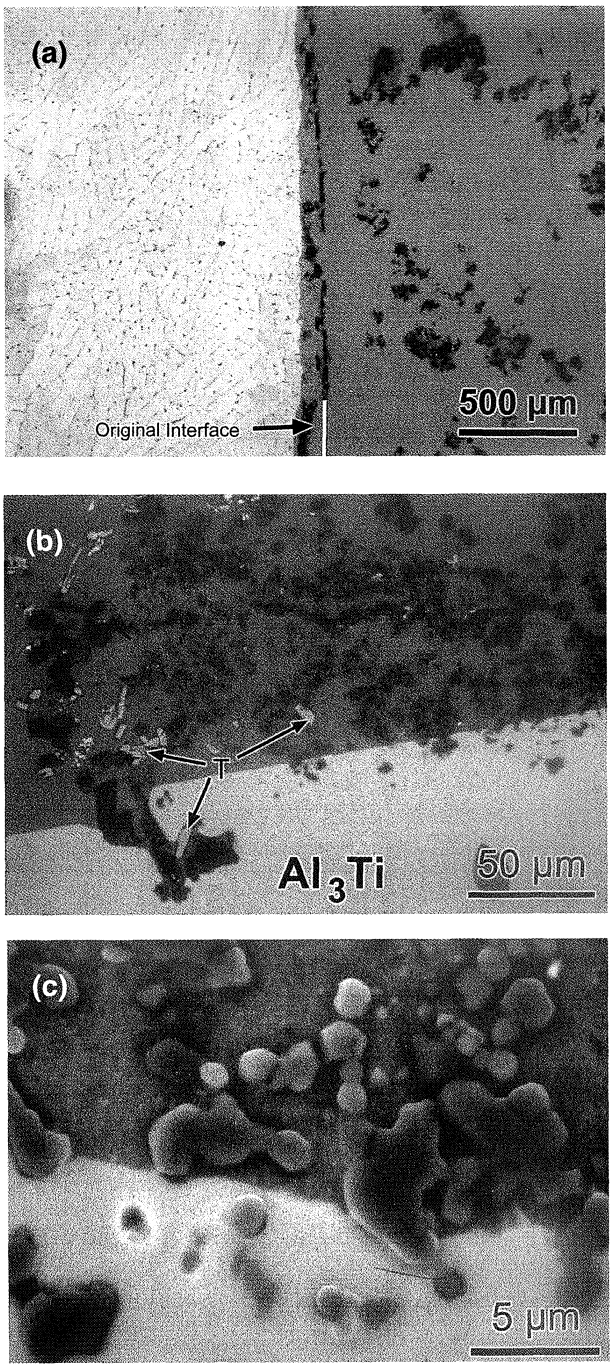

Figure 8. BEI + SEI micrographs of the diffusion couple obtained at different magnifications: a) Left side is Al_3Ti and right side, Al-B alloy containing 7.08 at % B. The dark gray phase on the right side corresponds to AlB_2 particles. b) Close up of the interface between Al_3Ti (lower side) and the Al-B binary alloy (upper side). c) Micrograph illustrating how the interface moved to the Al-B side of the diffusion couple.

Figura 8. Micrografías BEI + SEI del par de difusión, obtenidas a diferentes aumentos: a) El lado izquierdo es Al_3Ti y el lado derecho, una aleación Al-B conteniendo 7,08 % atómico de B. La fase gris oscura a la derecha corresponde a partículas de AlB_2. b) Detalle de la interfase entre Al_3Ti (lado inferior) y la aleación binaria Al-B (lado superior). c) Micrografía ilustrando cómo la interfase se movió hacia el lado con Al-B del par de difusión.

($T_m \cong 660$ °C). In figure 10 this proposed phase development is sketched along with a DTA cooling curve. T_u represents the temperature where only liquid aluminium and the solid substrates (Al_3Ti and TiB_2) are present; T_n is the temperature of early formation of solid α-Al phase on the potent substrates; T_u represents the temperature for undercooled α-Al phase formed on non-catalytic sites. The smallest and lowest signal at T_e may be due to undercooled Al + AlB_2 eutectic formation.

The reactivity of TiB_2 or $(Al,Ti)B_2$ with Al_3Ti in the presence of liquid aluminium led to the suspicion that boron atoms from the diborides could have dissolved into the *tI8* structure of Al_3Ti. The amount (furbished with a windowless detector) of dissolved boron could have occurred in levels below the detection limits of the EDS unit, which did not reveal any appreciable boron in the Al_3Ti side of the diffusion couple (Fig. 9). Despite that situation, dissolved boron atoms could have been present in an amount sufficient to alter the trialuminide lattice parameters as much as necessary to achieve a very low lattice mismatch with an Al matrix, as it occurred with silicon impurities in Al-Ti master alloys[6 y 7]. This appealing possibility required further exploration since it could have explained the enhanced catalytic effect of Al_3Ti when boron is present in the master alloy. The possible solid solution of boron in the trialuminide would have created a single-phase field extension into the Al-Ti-B phase diagram, as indicated in figure 2. To study this alternative explanation, experimental ternary alloys were investigated using accurate X-ray diffraction measurements of the lattice parameters *a* and *c* of the *tI8* trialuminide when boron is

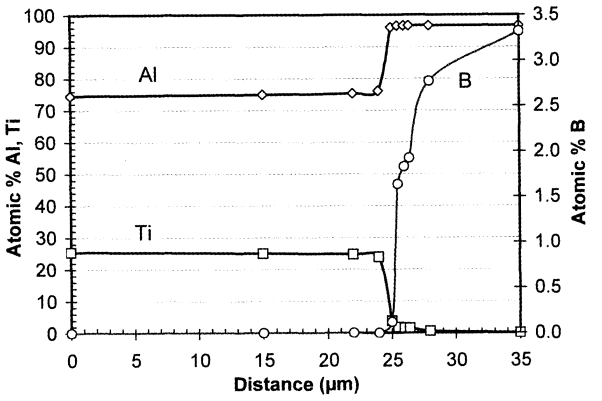

Figure 9. Concentration profile in the diffusion couple of figure 8a, as measured by EDS analysis.

Figura 9. Perfiles de concentración en el par de difusión de la figura 8a, obtenidos mediante análisis EDS.

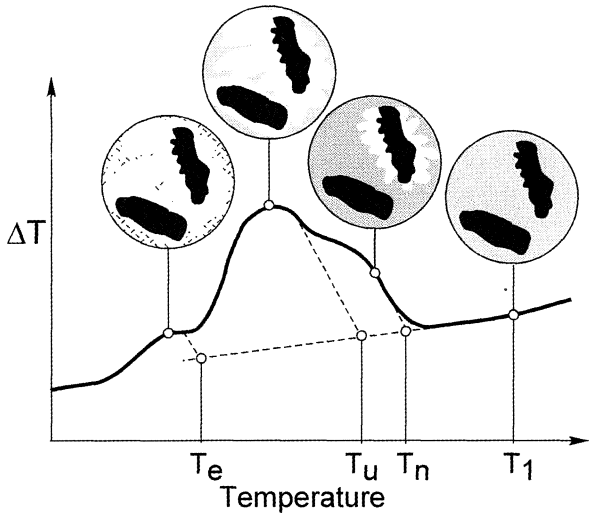

Figure 10. Schematic proposed phase development corresponding to the thermal signature of the experimental and commercial Al-Ti-B alloys, prepared based upon DTA and quenching studies.

Figura 10. Esquema propuesto del desarrollo de fases correspondientes a los resultados térmicos producidos por aleaciones experimentales y comerciales de Al-Ti-B, preparado en base a los estudios en DTA y temple.

present. The result of statistical analysis of the lattice parameters measurements for all the alloys indicated in figure 2 is presented in table I along with literature data for pure Al_3Ti phase. Noticeably, there are no statistically significant differences in lattice parameter between the Al_3Ti phase present in the experimental ternary alloy and the data reported in the literature[17-21]. Therefore, the hypothesis of a single-phase field extension of figure 2 was rejected: boron does not appear to dissolve into the trialuminide.

When the equilibrium Al-Ti-B phase diagram was modeled using a thermodynamic package and the ternary phase $(Al,Ti)B_2$ was taken into consideration, the isothermal sections in figure 11 were obtained at 700 °C and 400 °C; i.e. above and below aluminium solidification temperature. Clearly, it has been possible to include a ternary phase $(Al,Ti)B_2$ in equilibrium with the liquid phase (at 700 °C). Therefore, titanium diboride should be expected to dissolve some aluminium as the liquid cools and solidifies.

In a recent work by the author on MgB_2 - reinforced composites also containing AlB_2 (another AlB_2-like *hP3* tetragonal crystal structure[22]), powder mixtures containing magnesium diborides and high purity (Al) were compacted, sintered and arc-melted. Electron microscopy work detected thin diboride plates with a likely formula $Al_{1-x}Mg_xB_2$ according to X-ray microanalysis. This solubility is not entirely surprising due to the aforementioned affinity between AlB_2 and other diborides, including TiB_2 and MgB_2. Additionally, due to the low atomic numbers of magnesium and aluminium, both compounds have a mostly metallic bond, which differentiates them from other transition metal diborides, e.g. ZrB_2, NbB_2 and HfB_2, which have a strong covalent contribution to the atomic bonding, which results in higher melting points[23]. In the case of TiB_2 it is assumed that the titanium sites (hexagonal layers) can be substitutionally occupied by aluminium atoms, maintaining the boron atoms located in the (002) planes unaltered. At this point, there is an ongoing research investigating this issue.

Table I. Al_3Ti lattice parameters reported in the literaure and measured in the present investigation

Tabla I. Parámetros de red de Al_3Ti obtenidos de la literatura y medidos en la investigación presente

	a	c	c/a
Author	nm	nm	-
Raman *et al.*[17]	0.384	0.858	2.234
Miida *et al.*[18]	0.384	0.856	2.229
Norby *et al.*[19]	0.38537	0.85839	2.227
Shridharan *et al.*[20]	0.3846	0.8594	2.235
Tsunekawa *et al.*[21]	0.3853	0.8618	2.237
Present investigation	0.3849	0.8606	2.236

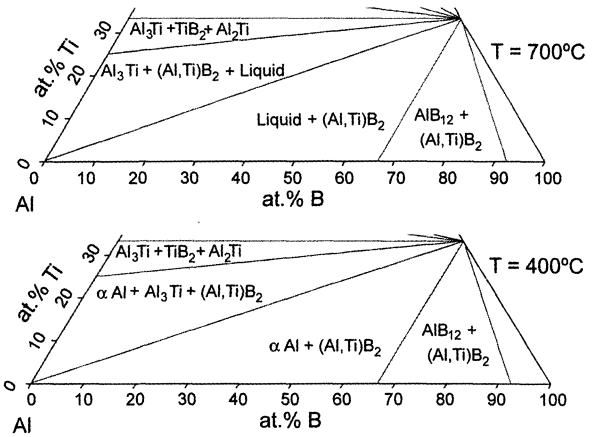

Figure 11. Partial isothermal sections of Al-Ti-B phase diagram computed at 700 °C (upper diagram) and 400 °C (lower diagram).

Figura 11. Secciones isotérmicas parciales del diagrama de fase Al-Ti-B calculado a 700 °C (diagrama superior) y 400 °C (diagrama inferior).

According to the phase diagram for Al-rich alloys containing more than roughly half as much boron in atomic percent as titanium, one should expect three phases before solidification (liquid, Al_3Ti and $(Al,Ti)B_2$) and upon solidification (αAl, Al_3Ti and $(Al,Ti)B_2$). This factor preconditions the melt, favoring the appearance of titanium aluminide in commercial grain refiners (usually with amounts of boron of 2.5 at % and of titanium of 2.8 at %). Further examination of the quenched samples displaying the offshoot-shaped α-Al phase (incipient dendrites) indicated the existence of diboride particles attached on the surface of the seemingly catalytic Al_3Ti substrates. Hence, it was conjectured that the ternary diboride rather than the trialuminide would be the actual catalytic particle. Since its presence is always associated with the trialuminide, this latter one appears as the actual substrate.

On the other hand, the diffusion couple experiments corroborated the high reactivity between Al_3Ti and a binary Al-B alloy even in the solid state. According to the phase diagrams in figure 11, some Al_2Ti could have been formed along with $Al_xTi_{1-x}B_2$ with x close to 1. In effect, as shown in figure 8b, this has been corroborated by the diffusion couple experiment. Additionally, figure 8a shows that the interface has moved into the Al_3Ti side as the titanium diffused into the aluminium diborides and released some aluminium. This effect is clearly observable in figure 8a where the α-Al region appears as if it moved into Al_3Ti phase.

In a recent work, *Limmaneevichitr and Eidhed*[24] attributed the well known fading of the effectiveness of Al-Ti-B grain refiners to settling of the catalytic particles; i.e. Al_3Ti and TiB_2 due to their higher densities. They detected macrosegregation of titanium and boron towards the bottom of tall aluminium castings. Accordingly, final grain size varies from the largest size at the top of samples to the finest size at the bottom. There is, nevertheless, a somewhat significant difference in density between Al_3Ti (3.16 g/cm^3) [25] and TiB_2 (4.51 g/cm^3 at room temperature) [26]. This difference would have caused a higher concentration of boron rather than titanium on the bottom of the specimens. On the other hand, AlB_2 with a density of 3.38 g/cm^3 at room temperature[27] or a ternary $(Al,Ti)B_2$ phase are much closer to the trialuminide and could have settled at a similar pace. There is an alternative explanation that also supports the findings in the present investigation. The attachment of $(Al,Ti)B_2$ onto the trialuminide particles has been proved in this research. It is possible that there is a coupled settling since the fine diboride particles are attached to the trialuminides (with larger volume and, hence, under the effect of larger sinking force) and both particles sink at the same rate.

5. CONCLUSIONS

Experimental and commercial Al-Ti-B alloys display similar thermal evolution upon solidification. Understandably, the only difference is a more energetic exothermic reaction for the formation of α-Al phase (nucleated on potent substrates) in the commercial alloy that contains a larger atomic fraction of aluminium.

The effect of titanium and aluminium diborides in the nucleation of aluminium was re-examined by trying to isolate the potent catalytic sites involved in aluminium heterogeneous nucleation. Contrary to some published research, the experimental results did suggest some solubility between TiB_2 and AlB_2, a factor also supported by thermodynamic modeling. This should not be surprising, as magnesium and some transition elements forming stable diborides with the *hP3* structure display solubility in the AlB_2 phase. Almost no TiB_2 or $(Al,Ti)B_2$ particles have been found away from the trialuminides in the emulsified samples. TiB_2 is already present when the Al_3Ti phase forms with almost no undercooling. Both statements may indicate that TiB_2 can be acting as nucleation sites for the trialuminide. This proximity would favor the close contact between Al_3Ti and TiB_2 to eventually give place to the diffusion of aluminium atoms into the *hP3* structure of TiB_2 to form $(Al,Ti)B_2$.

On the other hand, the possibility of some solubility of boron in the *tI8* structure of the titanium trialuminide was discarded by X-ray diffraction analysis of ternary Al-Ti-B alloys. This discovery directed the focus of the present investigation back to the diborides.

As indicated previously, in the presence of liquid aluminium, TiB_2 became less stable and often appeared associated with Al_3Ti particles. This was shown by different techniques including diffusion couple studies, and DTA and SEM studies.

Rapid quenching experiments showed the stability of TiB_2 at high temperature in liquid aluminium containing titanium, but this stability disappeared in the presence of Al_3Ti particles in the liquid. Diffusion couple studies with binary

Al-B alloys and pure Al_3Ti provided further evidence to support the lack of TiB_2 stability in contact with the trialuminide.

In summary, this work suggests that ternary diborides $(Al,Ti)B_2$ play an important role in the crystallization of aluminium, perhaps acting as the main catalytic substrate. As for practical aspects of grain refinement, this investigation helps to explain as well the fading effect by settling of trialuminide and diborides. To define the exact settling mechanism, additional research would be needed by analyzing the particles found at the bottom of a casting.

Acknowledgments

Partial support of the present project by the College of Engineering, Univ. of Puerto Rico-Mayagüez, is greatly appreciated. Additionally, the author would like to extend his gratitude to Dr. Fanyu Xie, from CompuTherm LLC, Wisconsin, USA, for his help in the thermodynamic modeling the Al-Ti-B phase diagram and to Prof. John H. Perepezko from the University of Wisconsin-Madison, USA, for his input in the analysis and interpretation of the results. The donation of master alloys by Milward Alloys, Inc., New York, USA, is kindly appreciated. $(Al, Mg)B_2$ studies are being conducted in collaboration with Prof. Eric E. Hellstrom from the University of Wisconsin-Madison and were supported by the National Science Foundation Grant No. DMR-00351449.

REFERENCES

[1] O.M. SUÁREZ, R.D. KENDRICK and C.R. LOPER JR., *Int. J. Cast Met. Res.* 13 (2000) 135-145.

[2] O.M. SUÁREZ, Ph. D. Thesis, Dept. of Materials Science and Engineering, University of Wisconsin-Madison, USA, 2000.

[3] J.E. GRUZLEZKI and B.M. CLOSSET, *The Treatment of Liquid Aluminum-Silicon Alloys*, American Foundry Society, Des Plaines, Illinois, USA, 1990, pp. 107-125.

[4] D.A. GRANGER, *Proc. Light Met. 1992*, San Antonio, Texas, USA, B. Welch (Ed.), ASM International, Materials Park, Ohio, USA, 1992, pp. 941-952.

[5] D.G. MCCARTNEY, *Int. Mat. Rev.* 35 (1989) 247-260.

[6] M.K. HOFFMEYER and J.H. PEREPEZKO, *Scri. Metall.* 22 (1988) 1143-1148.

[7] M.K. HOFFMEYER and J.H. PEREPEZKO, *Scri. Metall.* 23 (1989) 315-320.

[8] T. MIZOGUCHI, J.H. PEREPEZKO and C.R. LOPER JR., *AFS Trans.* 104 (1997) 89-94.

[9] M.M. GUZOWSKI, G.K. SIGWORTH and D.A. SENTNER, *Metall. Trans.* A 18A (1987) 603-619.

[10] X. LIU, X. BIAN and J. MA, *Proc. 7th Int. Conf. ICAA7*, Charlottesville, Virginia, 2000, E. A. Starke Jr., T.H. Sanders Jr. and W.A. Cassada (Eds.), Trans. Tech. Publ., Switzerland, 2000, pp. 384-389.

[11] P. SCHUMACHER, A.L. GREER, J. WORTH, P.V. EVANS, M.A. KEARNS, P. FISHER and A.H. GREEN, *Mater. Sci. Technol.* 14 (1998) 394-404.

[12] F. ZUPANIC and S. SPAIC, *Metallurgia* 53 (1999) 125-130.

[13] O.M. SUÁREZ, Master of Science Thesis, Dept. of Materials Science and Engineering, University of Wisconsin-Madison, USA, 1993.

[14] K.L. TEE, L. LU and M.O. LAI, *Mater. Sci. and Technol.* 17 (2001) 201-206.

[15] O.M. SUÁREZ, *J. Mech. Behav. Mater.* 12 (2001) 225-237.

[16] O.M. SUÁREZ and J. H. PEREPEZKO, *Proc. Light Met. 1992*, San Diego, California, 1992, E.R. Cutshall (Ed.), ASM *International*, Materials Park, Ohio, 1992, pp. 851-859.

[17] A. RAMAN and K. SCHUBERT, *Z. Metallk. de.* 56 (1965) 44-52.

[18] R. MIIDA, M. KASAHARA and D. WATANABE, *Jap. J. Appl. Phys.* 19 (1980) L707-L710.

[19] P. NORBY and A.N. CHRISTENSEN, *Acta Chem. Scand. Ser. A: Physical and Inorganic Chemistry* 40A (1986) 157-159.

[20] S. SHRIDHARAN, H. NOWOTNY and S.F. WAYNE, *Monatsh. Chem.* 114 (1983) 127-135.

[21] S. TSUNEKAWA and M.E. FINE, *Scri. Metall.* 16 (1982) 391-392.

[22] A. RAMAN, *Z. Metallk. de* 58 (1967) 179-184.

[23] P. VAJEESTON, P. RAVINDRAN, C. RAVI and R. ASOKAMANI, *Phys. Rev.* B 63 (2001) 045115-1-12.

[24] C. LIMMANEEVICHITR and W. EIDHED, *Mater. Sci. Eng.* A 349 (2003) 197-206.

[25] R.C. HANSEN and A. RAMAN, *Z. Metallk. de* 61 (1970) 115-120.

[26] E.A. KNYSHEV, *J. Less-Common Met.* 47 (1976) 273-278.

[27] E.J. FELTEN, *J. Am. Chem. Soc.* 78 (1956) 5977-5978.